Fibers and Polymers (2023) 24:4121–4128
https://doi.org/10.1007/s12221-023-00384-5

Online ISSN 1875-0052
Print ISSN 1229-9197

REGULAR ARTICLE

Characterization and Mechanism Analysis of Flexible UV Irradiated PAN-Based Carbon Fiber Membranes Prepared

Chao Hou[1] · Miao Yu[1] · Binjie Xin[1]

Received: 23 June 2023 / Revised: 25 September 2023 / Accepted: 1 October 2023 / Published online: 26 October 2023

Abstract

To enhance the flexibility of electrostatically spun PAN-based carbon nanofiber films for wearable textile applications, this study aimed to prepare PAN nanofiber films by incorporating the 1173 photoinitiator. Subsequently, UV irradiation, pre-oxidation treatment, and high-temperature carbonization processes were employed to develop PAN nanofiber films with improved mechanical properties. The results indicated that UV irradiation treatment significantly promoted the degree of pre-oxidation reaction in PAN nanofiber membranes. Thermal performance characterization demonstrated that UV irradiation reduced the initiation temperature of the cyclization reaction and mitigated the concentration of exothermic phenomena. Raman spectra analysis revealed increased graphitization in the carbon nanofiber film following UV irradiation, as evidenced by a decrease in the ID/IG value to 0.908. This suggests that UV irradiation facilitated stable carbonization and enhanced the graphitization of the carbon fiber within PAN nanofiber films. Moreover, the stress–strain curve indicated that the breaking strength of the nanofiber film reached 1.45 MPa after 20 min of UV irradiation while maintaining an elongation at a break of 3.5%, demonstrating its remarkable strength and toughness. The resulting flexible carbon nanofiber film holds great potential for medical textiles, filtration membranes, flexible capacitors, and more applications.

Keywords Carbon fiber · UV irradiation · High-temperature carbonization · Flexible · Wearable textile

1 Introduction

Carbon fibers are high-strength and lightweight materials with over 92 wt% carbon [1]. Surface treatments are often applied to carbon fibers to enhance their functionality and performance. These treatments include anodic oxidation [2], plasma treatment [3, 4], oxyfluorination [5], ozone treatment [6], fluorination [7], argon ion beam treatment [8–10], metal coating [11–14], and chemical treatment [15, 16]. These surface modifications find extensive applications in various industrial fields, such as adsorption [17, 18], detoxification [19], catalysis [20], adhesion or composites [21, 22], and electrochemistry [23, 24]. Due to their excellent electrical conductivity, thermal stability, and high specific surface area, carbon fibers are widely utilized in sensors, oil–water separation, air filtration, catalytic degradation, and heavy metal ion detection [25]. The main types of carbon fibers used in industrial production are polyacrylonitrile (PAN)-based carbon fibers, viscous-based carbon fibers, and asphalt-based carbon fibers. PAN-based carbon fibers are a promising precursor material due to their cost-effectiveness and high yield.

However, conventional electrostatically spun carbon nanofiber films are prone to brittleness and breakage, which hinder their applications in various fields [26]. Addressing this issue is crucial to expanding carbon nanofiber membranes' application range. In recent years, there has been significant research interest in flexible carbon nanofiber membranes, aiming to overcome their fragility and explore their potential applications in medical textiles, filtration membrane products, flexible capacitors, and other fields.

To obtain carbon fibers with excellent mechanical properties, pre-oxidation is commonly performed before the carbonization of polyacrylonitrile, resulting in a stable trapezoidal molecular structure. Previous studies have mainly focused on the thermal oxidation process of polyacrylonitrile. For instance, Shokrani Havigh et al. [27] researched the carbonization temperature for converting polyacrylonitrile precursor fibers into carbon fibers. Liu and Kumar [28]

✉ Binjie Xin
xinbj@sues.edu.cn

[1] School of Textiles and Fashion, Shanghai University of Engineering Science, Shanghai 201620, China

reported the relationship between processing conditions, chemical/physical structure, and tensile properties. However, the thermal oxidation process is time-consuming (2–3 h) and incurs high costs and energy consumption. As a result, alternative methods based on radiation oxidation have been developed, which induce changes in the polymer structure and positively impact the mechanical strength of polyacrylonitrile-based carbon fibers. Nevertheless, further improvements are necessary to enhance their convenience and environmental friendliness. Shortening the pre-oxidation phase of polyacrylonitrile fibers remains a focal point of research. Irradiation treatments have significantly affected polyacrylonitrile's molecular chain structure and thermal properties, forming free radicals and small molecules that can result in cross-linking or chain breakage.

In this study, 1173 was used as a photoinitiator to prepare a polyacrylonitrile spinning solution, which was then subjected to electrostatic spinning to obtain the primary fibrous film. Subsequently, the film underwent UV irradiation and thermal oxidation treatment to achieve an intermediate film with a stable structure. Finally, high-temperature carbonization was conducted to obtain the final flexible carbon nanofiber membrane (FCNF) with sufficient mechanical strength. By investigating different UV irradiation times, it was found that UV irradiation treatment promoted the degree of pre-oxidation reaction of PAN nanofiber membranes and facilitated the stable carbonization of PAN nanofiber membranes and the best mechanical properties of carbon fiber membranes were obtained at 20 min of UV irradiation.

2 Experimental

2.1 Materials

Polyacrylonitrile (PAN, Mw = 150,000), *N*,*N*-dimethylformamide (DMF, purity 99.5%), anhydrous ethanol (CH_3OH), and nitrogen (N2) were obtained from Sinopharm Chemical Reagent Co. The photoinitiator 1173 (2-hydroxy-2-methylpropiophenone, purity > 96.0%) was purchased from Toshiyaki (Shanghai) Chemical Industry Development Co. All reagents were used as received without further purification.

2.2 Preparation of Carbon Fiber Membranes

Firstly, a PAN spinning solution was prepared by weighing a specific amount of photoinitiator 1173 and PAN powder and adding them to DMF. The mass fraction of PAN in the spinning solution was set at 15%, with the photoinitiator 1173 mass being 2% of the PAN powder mass. The solution was then stirred on a magnetic stirrer for 8 h to achieve uniformity. Subsequently, the spinning solution was loaded into a 5 mL syringe, and a metal nozzle was connected to a rigid tube and hose. The metal receiver roller was wrapped with aluminum foil, and a high-voltage power supply was connected in preparation for electrostatic spinning. The electrostatic spinning process was conducted with a feed rate of 1.0 mL h^{-1}, a voltage of 19 kV, and a distance of 15 cm between the needle and the roller collector. The humidity inside the electrostatic spinning chamber was maintained at 75 ± 5%, and the temperature was set at 20 ± 2 °C. After 4 h of spinning, the primary film was detached and dried in a vacuum oven at 60 °C for 8 h. The dried films were then cut into 5 equal sizes and exposed to UV light in a PANTONE chamber for 0, 5, 10, 20, and 30 min, respectively, resulting in samples named UV-0, UV-5, UV-10, UV-20, and UV-30. Similarly, the samples were pre-oxidized for 45, 75, and 105 min, and the exact UV light treatment durations were applied. The carbon film subjected to 5 min of UV light irradiation and 105 min of pre-oxidation was denoted as UV-5–105—other samples named in this way. Finally, the pre-oxidized films were trimmed to appropriate sizes, placed in a quartz boat, and carbonized in a tube furnace. The carbonization process involved a temperature ramp from 50 to 1000 °C at a heating rate of 5 °C/min, with a 2-h holding time at the final temperature. Figure 1 presents the flow chart depicting the preparation of carbon fiber films.

2.3 Characterization

The morphology of the samples was examined by SEM (Zeiss Gemini 300). ImageJ's image processing program was used to measure the fiber diameter and membrane porosity. FTIR (Spectrum Two, USA)) analyzed the molecular chain

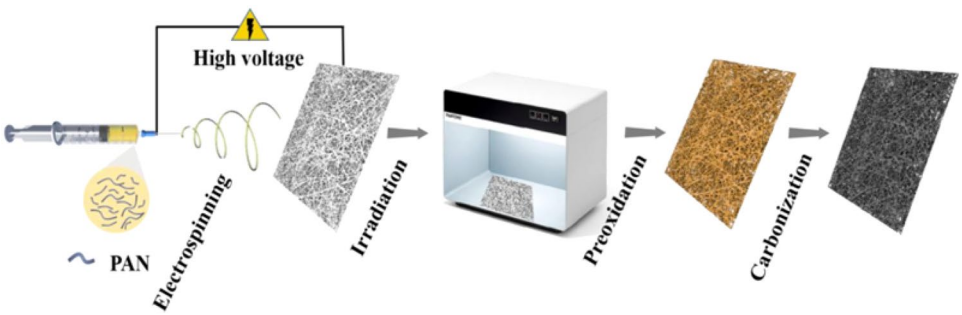

Fig. 1 Flow chart of carbon fiber preparation

structures. The extent of reaction (EOR) was measured by Eq. (1). The mechanical properties of the nano-fibrous membranes were evaluated at a strain rate of 2 mm/min using an XS (08) XT-2 Single Fiber Strength Tester (Shanghai Xusai Instruments Co.). The FCNF oscillated in the ultrasonic device (SK2200GT, Shanghai Kudos Ultrasonic Instrument Co., Ltd.) for a certain period to demonstrate the strength of the membranes. Wide-angle X-ray diffraction (XRD) analysis was performed using a Bruker D8 Advance (Cu Kα irradiated radiation) diffractometer. The Raman spectra were acquired on a Renishaw Raman via spectrometer. The thermal properties of the samples were determined by differential scanning calorimeter DSC4000 (Perkin Elmer, USA) and thermogravimetric analysis (TGA4000, PerKin Elmer, USA).

$$\mathrm{EOR} = \frac{I_{1600}}{I_{1600} + I_{C\equiv N}} \tag{1}$$

$I_{C\equiv N}$ indicates the intensity of the absorption peak of the cyanide group, and I_{1600} suggests the intensity of the absorption peak of the conjugated C=N group at 1600 cm^{-1}.

3 Results and Discussions

3.1 Morphology of Carbon Nanofibers

Figure 2(a–c, e, f) displayed SEM images of carbonized nanofiber films after various durations of UV irradiation treatment, corresponding to irradiation times of 0 min, 5 min, 10 min, 20 min, and 30 min, respectively. Figure 2f presents the corresponding distribution of carbon nanofiber diameters. Figure 2g featured the SEM image of the PAN-carbonized nanofiber membrane, while Fig. 2d depicted the corresponding distribution of carbon nanofiber diameters. Examining Fig. 2g, it becomes evident that the surface of the PAN-based carbon fibers was smooth and straight, displaying a disordered arrangement among the fibers, with a diameter of approximately 253 nm. Figure 2(a–c, e, f) demonstrated that carbon nanofibers subjected to different UV irradiation times had slightly roughened surfaces, exhibited similar apparent morphologies with almost no differences, and displayed fiber diameters that were uniformly distributed in the range of 200–250 nm.

3.2 Structure of Carbon Nanofibers

The PAN virgin fiber membranes were subjected to UV irradiation for various durations and subsequently pre-oxidized in an air atmosphere for 45 min, 75 min, and 105 min, respectively. The FTIR spectra were acquired using a Fourier infrared spectrometer, as depicted in Fig. 3. Figure 4 showed the PAN nanofiber film's color change at different pre-oxidation times at 250 °C. The degree of pre-oxidation reaction was determined using the provided formula, as presented in Table 1.

The stretching vibration absorption peak of –C≡N at 2245 cm^{-1} and the absorption peak corresponding to $–CH_2$ at 1454 cm^{-1} exhibited thin and sharp profiles, while the intensity of the C=N and C=C conjugate stretching vibration peaks at 1600 cm^{-1} was weak. This indicates the incipient cyclization and dehydrogenation reactions, suggesting that the response was at an early stage. Concurrently, the physical appearance of the 45-min pre-oxidation sample displayed a faint yellow color, resembling that of the primary fiber film (Fig. 4), which was corroborated by the IR spectra. Despite being in the early stages, the calculated EOR values demonstrated that UV irradiation had a beneficial influence on pre-oxidation.

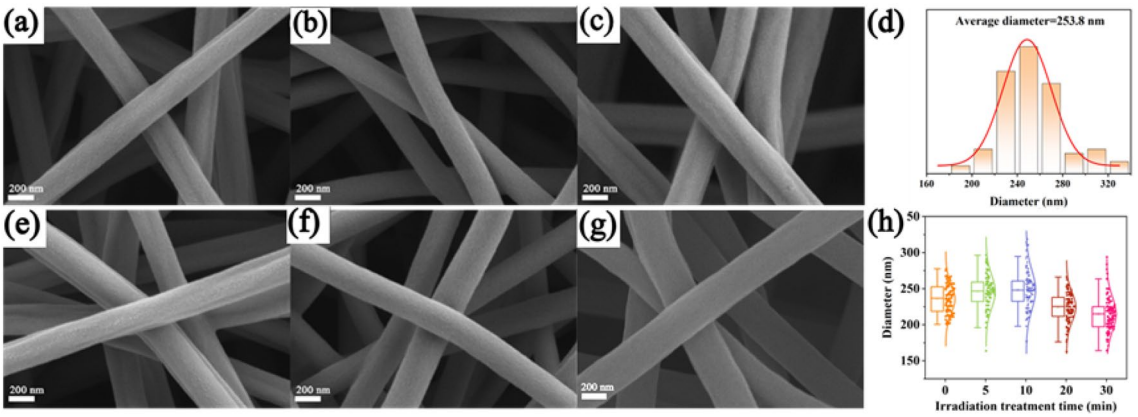

Fig. 2 **a**–**c**, **e**, **f** Carbonized nanofiber membranes after UV irradiation for different times, **g** PAN carbonized nanofiber membrane, **d** diameter distribution of pure polyacrylonitrile carbonized nanofibers, **h** diameter distribution of carbonized nanofibers after UV irradiation at different times

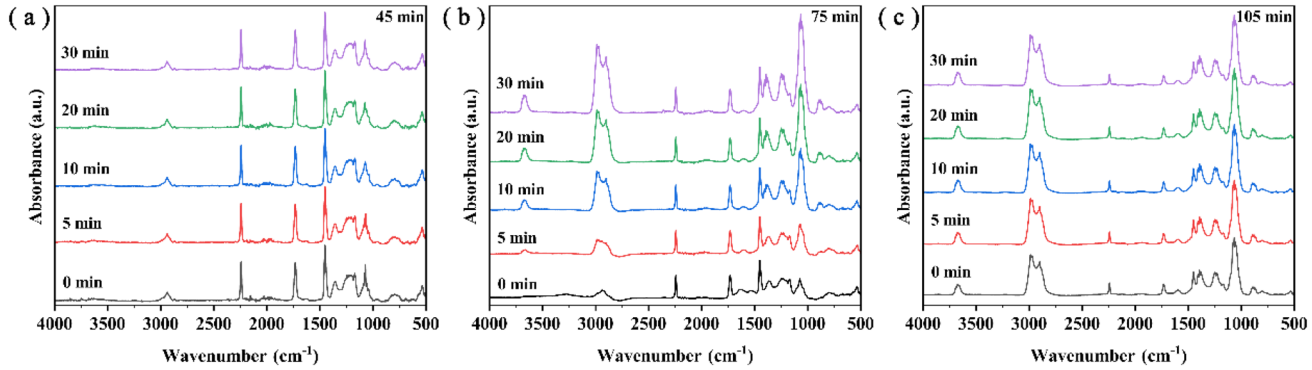

Fig. 3 Different times of UV irradiation of PAN fiber membrane after **a** pre-oxidation for 45 min, **b** pre-oxidation for 75 min, and **c** pre-oxidation for 105 min

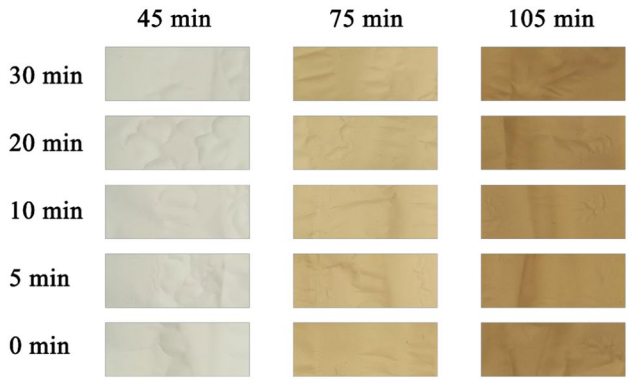

Fig. 4 Color change of PAN nanofiber membrane at different times of pre-oxidation at 250 °C

Table 1 The degree of response is calculated from FTIR plots

Time (min)	0	5	10	20	30
45	0.5419	0.5453	0.5387	0.5494	0.5325
75	0.5711	0.5745	0.5746	0.5762	0.5702
105	0.5817	0.5843	0.5855	0.5875	0.5850

Following 75 min of heating, the intensity of the –C≡N absorption peak considerably decreased, while the absorption peak of C=N gradually intensified, indicating further progress in the cyclization reaction. The physical appearance of the 75 min pre-oxidation sample exhibited a light-yellow color, and the EOR values listed in Table 1 were all higher compared to the 45 min heating, indicating a more profound pre-oxidation reaction for the nanofiber membrane with increased heating time under the same irradiation period. As the UV irradiation time increased, the EOR value initially increased and then decreased. This can be attributed to the fact that prolonged UV irradiation detrimentally affected the macromolecular chain structure of PAN itself, negatively impacting the subsequent pre-oxidation process. As the heating time increased, the physical appearance exhibited a darker yellow color, as exemplified by the 105 min pre-oxidation sample in Fig. 4. In conclusion, appropriate UV irradiation treatment enhanced the reactivity of the PAN nanofiber film within the same pre-oxidation duration.

3.3 Mechanical Properties

Based on the combination of the EOR values and the pre-oxidized fibers' physical diagram, the 105 min pre-oxidized sample exhibited a relatively more adequate reaction. Consequently, other properties were further investigated. The stress–strain curves of carbon nanofiber films with different UV irradiation times are shown in Fig. 5a. Notably, UV-0–105 could not be characterized due to its brittleness. Of particular interest is the UV-20–105 sample, which exhibited the most favorable mechanical properties at a carbonization temperature of 1000 °C. It maintained an elongation at a break of 3.5% and achieved a breaking strength of 1.45 MPa, indicating considerable strength and toughness. Although UV-30–105 attained a higher elongation at a break of 3.7%, its breaking strength was only 0.4 MPa. The results for UV-5–105 and UV-10–105 were slightly better but still fell short. This is mainly because the photoinitiator 1173 is excited by UV irradiation, which causes PAN to produce free radicals and induces the formation of cross-links between molecular chains, improving the material's mechanical properties. Prolonged UV irradiation may trigger molecular chain breakage or chain depolymerization reaction, Therefore, the mechanical properties decreased after 30 min irradiation time. As anticipated, UV irradiation treatment significantly influenced the mechanical properties, with an irradiation time of 20 min deemed suitable.

In Fig. 5b, the ultrasonic oscillation experiment was conducted to qualitatively assess the strength of the carbon nanofiber film by simulating external destructive forces

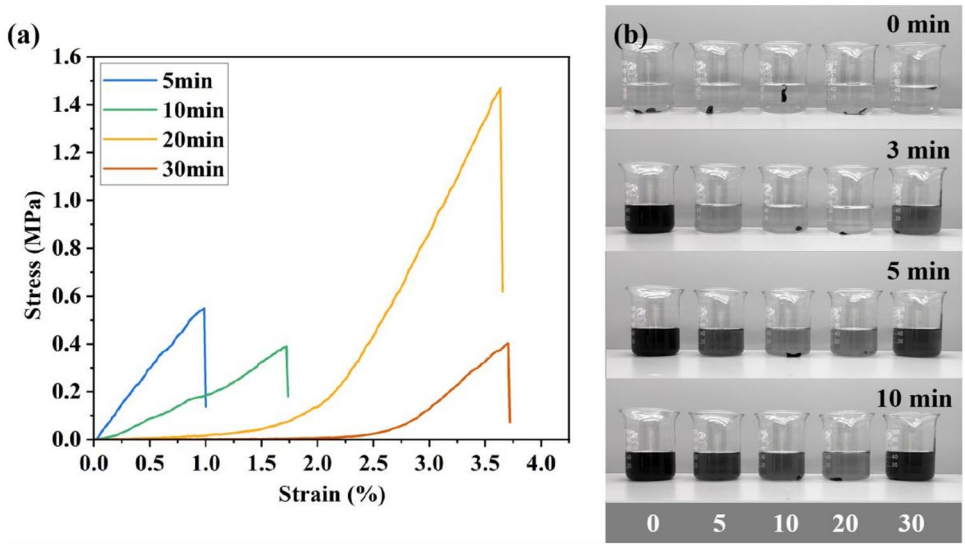

Fig. 5 **a** Stress–strain curve and **b** ultrasonic oscillation test of carbon nanofiber membrane

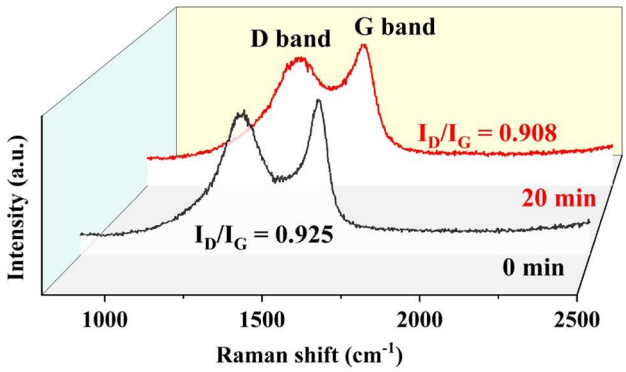

Fig. 6 Raman spectrogram of carbon nanofiber membrane

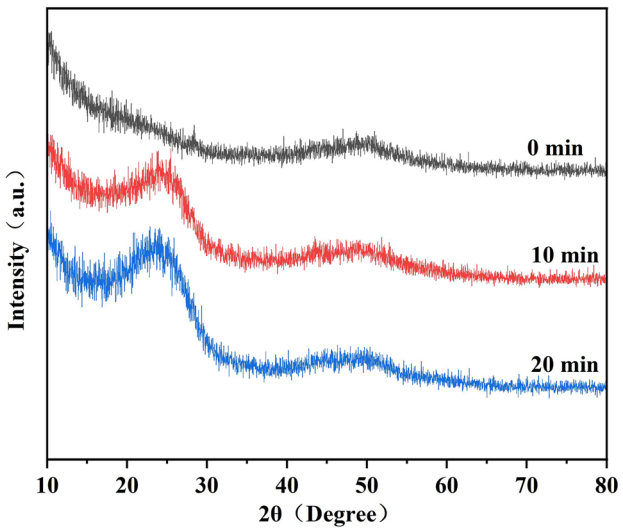

Fig. 7 XRD plots of carbon nanofiber membranes

using ultrasonic waves. Visual observations revealed varying degrees of damage to UV-0–105 and UV-30–105 within 3 min. After 5 min, the beakers containing UV-5–105, UV-10–105, and UV-20–105 showed slight cloudiness, indicating partial breakage of the carbon nanofiber film. By the spanning time of 10 min, the distilled water in the UV-20–105 beaker was relatively clear, while the other samples had utterly disintegrated. This experiment indirectly demonstrated the excellent mechanical properties of UV-20–105.

3.4 Crystallinity Analysis

Raman spectroscopy was utilized to examine the crystalline structure of the various carbon fibers. The Raman spectra presented in Fig. 6 showcased two bands: the "D-peak" associated with disordered carbon structures and the "G-peak" associated with well-organized graphite structures. A lower ID/IG value indicated a more ordered carbon fiber construction, while a higher ID/IG value indicated the opposite [29]. The ID/IG values before and after UV irradiation were depicted in Fig. 6, reflecting the alteration in the crystalline state of the carbon nanofiber surface. The ID/IG values of the carbon nanofiber films decreased from 0.925 without treatment to 0.908 after UV irradiation, indicating that the stable carbonization of the PAN nanofiber films was facilitated, and the graphitization of the carbon fibers was enhanced.

In Fig. 7, broad diffraction peaks were observed around $2\theta = 26°$ and 45°, corresponding to the characteristic peaks of the graphite (002) and (100) crystals on the surface. This indicated that the sample had undergone partial graphitization following high-temperature carbonization. The appearance of these graphite crystal facets may be due to the crystal structure adjustment triggered by UV irradiation, which

promotes the growth of graphite crystal facets. A leftward shift of the XRD curves was observed in the figure as the UV irradiation time increased, suggesting more significant cell parameters and increased crystalline surface spacing. The increase in cell parameters may be related to the action of UV light, which may lead to the breaking or structural change of some bonds in the polyacrylonitrile (PAN) molecule, affecting the crystal size and cell parameters. The grain size was calculated to be 10.59 nm for UV-10–105 and 10.37 nm for UV-20–105 using X-ray diffraction analysis, according to the Debye–Scherrer Eq. (2). These changes in grain size may be due to UV irradiation triggering chain depolymerization reactions in the PAN molecules, leading to adjustments in the crystal structure and changes in grain size. The changes in grain size may affect the number and distribution of grain boundaries, which in turn affects the mechanical properties of the samples. The grain size fundamentally reflected the size of the grain boundary region. A finer grain size resulted in more grain boundaries, increased interlacing, larger grain boundary areas, and a more uniform distribution of deformation among the grains.

Consequently, this facilitated reduced stress concentration, enhanced crack avoidance, and improved strength and toughness of the material. The material's mechanical properties were closely related to its crystallization [30]. Therefore, it was anticipated that the fibers subjected to 20 min of UV irradiation would exhibit superior mechanical properties.

$$D_{hkl} = \frac{k\lambda}{\beta \cos\theta_{hkl}} \tag{2}$$

where λ is the wavelength of X-rays, θ is the diffraction angle, β is the width at half height (FWHM) of the diffraction peak at 2θ, and $k = 0.89$ is a constant.

3.5 Thermal Performance Analysis

The thermal properties of PAN nanofiber films under different UV irradiation times were analyzed using DSC spectra (Fig. 8). Since the experiments were conducted under an N2 atmosphere, only the cyclization reaction occurred, while no indication oxidation reaction occurred. As depicted in Fig. 8, PAN exhibited a narrow exothermic peak, indicating the rapid release of a significant amount of reaction heat within a short period. This phenomenon can lead to the breakage of PAN molecular chains and is not conducive to producing high-performance carbon fibers. However, with increasing UV irradiation time, the DSC curve broadened and shifted to the left, indicating that UV irradiation treatment could induce cyclization and moderate the exothermic reaction. The enthalpy of the

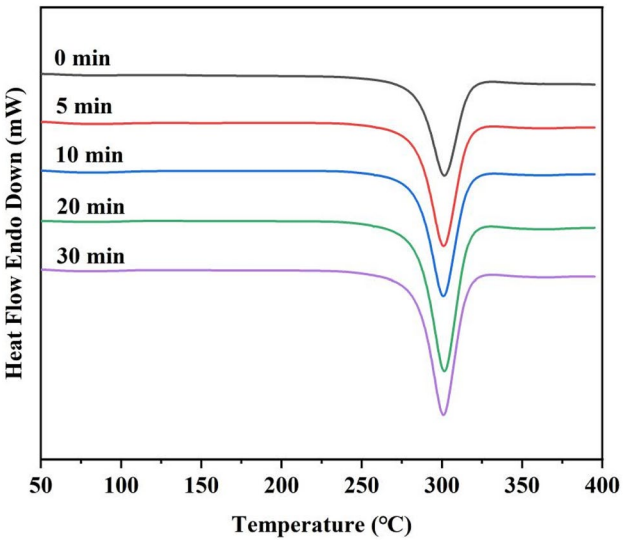

Fig. 8 DSC curves under N_2 atmosphere with different UV irradiation times

DSC exotherm under N2 conditions increased with longer UV irradiation time, as presented in Table 2, with UV-20 exhibiting the highest enthalpy of 686.13 J/g, suggesting a higher extent of nitrile group cyclization. This can be attributed to the excitation of more radicals and the promotion of the cyclization reaction by UV irradiation. These results confirm that UV irradiation before pre-oxidation can enhance the extent of the pre-oxidation response and alleviate the concentrated exothermic effect caused by the cyclization reaction during pre-oxidation treatment.

Figure 9 illustrates PAN fibers' thermogravimetric (TG) curves under a nitrogen atmosphere for varying UV irradiation durations. The figure reveals three distinctive weight loss stages for PAN fibers. The initial stage occurs within the temperature range of 94–130 ℃, attributed primarily to water evaporation. The subsequent stage spans from 310 to 480 ℃, during which both UV-irradiated and non-irradiated PAN fibers exhibit significant weight reduction, ranging from 36 to 44%. Remarkably, the PAN fiber subjected to 20 min of UV irradiation displays the swiftest weight loss within this range, primarily attributed to cyclization and dehydrogenation reactions. The final stage occurs at temperatures ranging from 480 to 800 ℃, with a deceleration in fiber weight loss. During this phase, cyclized molecular chains within the fiber manifest increased stability, whereas uncyclized or cross-linked molecular chains undergo thermal cracking reactions. These findings prove that UV irradiation effectively instigates rapid cyclization reactions within fibers by generating free radicals through chain breakage.

Table 2 Temperature and enthalpy of cyclization reaction at different UV irradiation times

Time of UV irradiation (min)	Time of pre-oxidation (min)	The temperature of cyclization starting (℃)	Temperature of cyclization peak (℃)	ΔH ($J \cdot g^{-1}$)
0	105	235.37	301.65	456.46
5	105	235.03	301.06	579.23
10	105	235.01	300.75	589.21
20	105	234.78	300.88	686.13
30	105	234.37	300.02	659.50

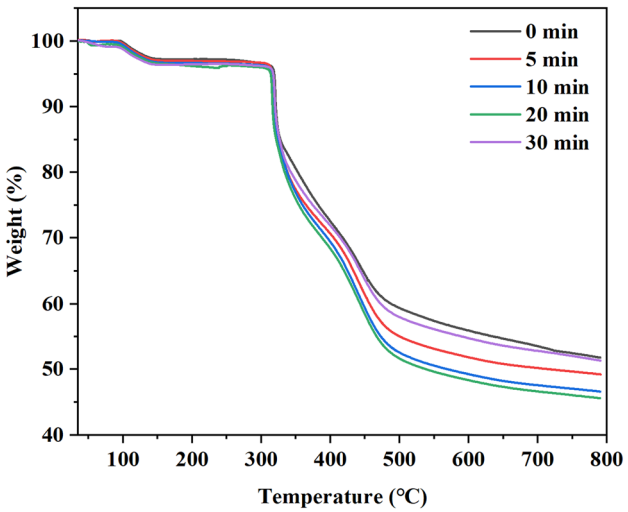

Fig. 9 TG curves under N_2 atmosphere with different UV irradiation times

3.6 Mechanistic Analysis

Previous studies have substantiated that UV irradiation on PAN generates free radicals, facilitating cross-linking between PAN molecular chains [31]. To a certain degree, this cross-linked structure hampers the disorientation of PAN nanofibers at elevated temperatures, thereby positively influencing the mechanical properties of CNF films [28]. The photoinitiator 1173 is activated by UV irradiation, resulting in its conversion to excited state molecules or ions. These excited state molecules or ions can trigger the breaking of specific bonds in the polyacrylonitrile molecule, generating free radicals with unpaired electrons. Figure 10 illustrates that oxygen in the ambient air reacts with the free radicals on the surface of PAN molecules, promoting cross-linking and initiating cyclization reactions. UV irradiation expedites the conversion of –C≡N to –C=N, resulting in a lowered starting temperature for the PAN cyclization reaction. During the pre-oxidation stage of PAN, cyclization, oxidation, and cross-linking reactions constitute the cyclization process. However, suppose the exothermic reaction is excessively concentrated. In that case, it can give rise to surface defects in the fibers and establish a skin–core structure, ultimately impeding sufficient pre-oxidation and adversely affecting the mechanical properties of the resulting carbon fibers.

4 Conclusion

In this study, a series of processes, including electrostatic spinning, UV irradiation, pre-oxidation, and carbonization, were employed to prepare flexible carbon nanofiber membranes with desirable mechanical strength using polyacrylonitrile (PAN) nanofiber membranes as the starting material. The findings demonstrated that UV irradiation treatment enhanced the degree of pre-oxidation reaction, promoted graphitization, reduced surface defects, and increased the number while decreasing the size of grains in PAN nanofiber membranes. The DSC analysis revealed an increase in exothermic enthalpy and broadening of peak shape with prolonged UV irradiation time. Notably, the highest enthalpy recorded for UV-20 was 686.13 J/g, which provided evidence that UV irradiation before pre-oxidation facilitated

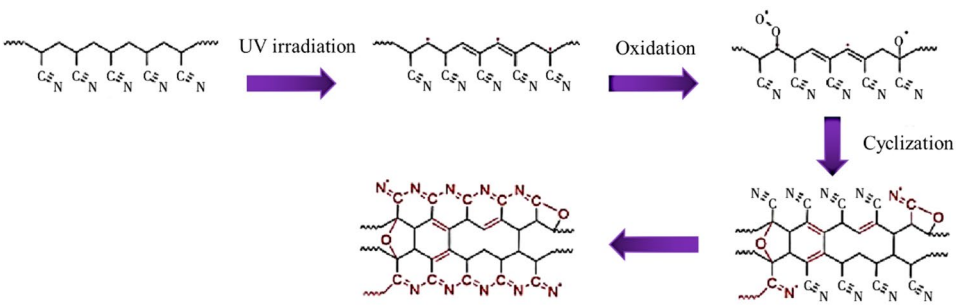

Fig. 10 Mechanism of the pre-oxidation reaction of PAN molecules under UV irradiation

the pre-oxidation process. The toughening mechanism of PAN-based carbon nanofiber films through UV irradiation was elucidated by analyzing the changes in PAN molecular structure and molecular chains, leading to the generation of free radicals on PAN fibers. This initiates cyclization reactions and other processes at lower temperatures, broadening the temperature range in which exothermic reactions occur and mitigating their concentration. Consequently, the PAN fibers achieve stable and adequate pre-oxidation, resulting in improved mechanical properties of the carbon nanofiber film. These findings offer valuable insights for advancing flexible carbon nanofiber film research.

Acknowledgements This project was funded by the National Natural Science Foundation of China (Grant No. 11702169) and Class III Peak Discipline of Shanghai—Materials Science and Engineering (High-Energy Beam Intelligent Processing and Green Manufacturing) (Project No.19YF1417900).

Data Availability Statement The data supporting the results of this study are presented in their entirety in the manuscript. These data are available from the authors upon reasonable request.

Declarations

Conflict of interest The authors certify that none of their known financial conflicts of interest or close personal ties might have appeared to have influenced the research presented in this study.

References

1. D. Gizik, C. Metzner, P. Middendorf, In: *20th International Conference on Composite Materials (ICCM)*, Copenhagen (2015)
2. Y. Fu, Y. Lu, T. You, J. Wu, W. Cao, Surface and interface. Analysis **51**(8), 798 (2019)
3. H. Lee, G. Kim, K. Kim, H. Kim, D.U. Kim, J. Mater. Eng. Perform. **32**(1), 415 (2023)
4. J. Xiao, X. Zhang, Z. Zhao, J. Liu, Q. Chen, X. Wang, ACS Omega **7**(13), 10963 (2022)
5. Y.-J. Yim, K.-M. Bae, S.-J. Park, Macromol. Res. **26**(9), 794 (2018)
6. J. Li, Iran. J. Chem. Chem. Eng. Int. Engl. Ed. **29**(1), 141 (2010)
7. J.-C. Agopian, O. Teraube, M. Dubois, K. Charlet, Appl. Surf. Sci. **534**, 147647 (2020)
8. A.M. Borisov, N.G. Chechenin, V.A. Kazakov, E.S. Mashkova, M.A. Ovchinnikov, Nucl. Instrum. Method Phys. Res. Sect. B Beam Interact. Mater. Atoms. **460**, 132 (2019)
9. V.A. Anikin, A.M. Borisov, A.V. Makunin, E.S. Mashkova, M.A. Ovchinnikov, Phys. At. Nucl. **81**(11), 1547 (2018)
10. H. Maier, M. Rasinski, U. von Toussaint, H. Greuner, B. Boeswirth, M. Balden, S. Elgeti, C. Ruset, G.F. Matthews, Phys. Scripta. **T167**, 014048 (2016)
11. J.-J. Sha, Z.-Z. Lu, R.-Y. Sha, Y.-F. Zu, J.-X. Dai, Y.-Q. Xian, W. Zhang, D. Cui, C.-L. Yan, Trans. Nonferr. Metals Soc. China. **31**(2), 317 (2021)
12. V.A. Nelyub, S.Y. Fedorov, G.V. Malysheva, A.A. Berlin, Fibre Chem. **53**(4), 252 (2021)
13. G.T. Lee, Y.K.I. Cho, W.S. Kim, J. Y. Kim. **70**(7), 1022 (2021)
14. B. Du, S. Zhou, X. Zhang, C. Hong, Q. Qu, Surf. Coat. Technol. **350**, 146 (2018)
15. S. N. M. Salleh, N. M. Zainon, M. Z. Abdullah, The Effect of Oleic Acid as Post Spinning Treatment on Tensile strength of Polyacrylonitrile Fibers, vol. 1901. In 3rd Advanced Materials Conference (AMC), Langkawi (2016)
16. D. Chukov, S. Nematulloev, M. Zadorozhnyy, V. Tcherdyntsev, A. Stepashkin, D. Zherebtsov, Polymers **11**(4), 684 (2019)
17. B. Petrovic, M. Gorbounov, S. Masoudi Soltani, Micropor Mesopor Mater. **312**, 110751 (2021)
18. Z. Wang, W. Xu, F. Jie, Z. Zhao, K. Zhou, H. Liu, Sci. Rep. **11**(1), 16878 (2021)
19. B.-J. Kim, K.-M. Bae, H.-M. Lee, S.-J. Kang, S.-J. Park, J. Nanomater. **16**, 328 (2016)
20. W.-K. Jo, S. Karthikeyan, M.A. Isaacs, A.F. Lee, K. Wilson, S.-H. Shin, J.-H. Lee, M.-K. Kim, B.-S. Park, G. J. J. O. T. T. I. O. C. E. Sekaran. **74**, 289 (2017)
21. S.P. Kumar, K. Jayanarayanan, M. Balachandran, Compos. Part B Eng. **253**, 110560 (2023)
22. Z. Zhang, X. Li, S. Jestin, S. Termine, A.-F. Trompeta, A. Araújo, R. M. Santos, C. Charitidis, H. J. P. Dong. **13**(20), 3457 (2021)
23. N. Sivaraman, V. Duraisamy, S.M.S. Kumar, R. J. C. Thangamuthu. **307**, 135771 (2022)
24. F. Ding, G. Zhang, C. Chen, S. Jiang, H. Tang, L. Tan, M. J. A. A. E. M. Ma. **3**(2), 761 (2021)
25. F. Cesano, M.J. Uddin, K. Lozano, M. Zanetti, D. J. F. i. M. Scarano. **7**, 219 (2020)
26. S. Mallakpour, and E. J. C. E. J. Khadem. **302**, 344 (2016)
27. R. Shokrani Havigh, H. Mahmoudi Chenari, Sci. Rep, **12** (1), 10704 (2022)
28. S.-Y. Son, A.Y. Jo, G.Y. Jung, Y.-S. Chung, S. Lee, J. Ind. Eng. Chem. **73**, 47 (2019)
29. P. Feng, G. Song, X. Li, H. Xu, L. Xu, D. Lv, X. Zhu, Y. Huang, L. Ma, J. Coll. Interface Sci. **583**, 13 (2021)
30. H. Yuan, Y. Wang, H. Yu, Z. Wei, B. Ge, Y. Mei, J. Wuhan Univ. Technol. Mater Sci. Ed. **26**(3), 449 (2011)
31. A.Y. Jo, S.H. Yoo, Y.-S. Chung, S. Lee, Carbon **144**, 440 (2019)